# Comparative Study of Simulated and Quantum Annealing for the Travelling Salesman Problem

Frederick Bullard
L3 Computing Project, Department of Physics, Durham University
Submitted: 15th March 2024

Solving combinatorial optimisation (CO) problems efficiently is an important challenge that spans various domains. In this report, we investigate and compare two prominent meta-heuristic approaches to tackle CO problems: simulated annealing (SA) and quantum annealing (QA). We use a 16-city instance of the Travelling Salesman Problem (TSP) as a test example and solve it via standard Monte Carlo SA and path-integral Monte Carlo (PIMC) QA. We determine the range of initial temperature $T_0$ for SA, as well as the ranges of Trotter number $P$ and ambient temperature $T$ for QA, that yield the most efficient and accurate results through studies of the dependence of the final residual length on each method's parameters. The superiority of PIMC QA relative to SA is demonstrated, for this TSP, with a study of the dependence of the final residual length on the total number of Monte Carlo steps. These results suggest QA could be an even better general-purpose CO meta-heuristic than SA. Future areas of investigation for QA and quantum optimisation as a whole are suggested.

## I. INTRODUCTION

Combinatorial optimisation (CO) is the act of finding the arrangement of a discrete set of objects that minimises a given cost function subject to a set of constraints. Generally, CO problems are difficult to solve as the space of possible solutions can be huge, making exhaustive search intractable. For such problems, we must resort to more specialised algorithms that rule out large parts of the solution space, or meta-heuristics that yield approximate solutions in a fraction of the time [1]. Two popular meta-heuristics are simulated annealing (SA) and quantum annealing (QA).

SA, first introduced in 1983 by Kirkpatrick et al., is a classical optimisation algorithm. Its name comes from the annealing process in metallurgy, where a metal is heated and then cooled in a controlled fashion to reach a low-energy crystalline state. SA mimics this cooling process, simulating thermal fluctuations to escape local minima and explore the solution space efficiently [2].

QA, on the other hand, uses quantum fluctuations provided by a transverse magnetic field to escape local minima. Like the temperature in SA, this field is slowly reduced to zero over the course of the annealing. The main advantage of exploiting quantum fluctuations over thermal fluctuations comes from the ability of quantum systems to tunnel into areas that are classically forbidden. As the field is reduced, the system explores lower energy regions until arriving at a final state [3].

In 2002, inspired by the experimental work of Brooke et al. who, a year earlier, demonstrated that QA performs better than thermal annealing in preparing the ground state of the spin-$1/2$ disordered Ising ferromagnet $\mathrm{LiHo}_{0.44}\mathrm{Y}_{0.56}\mathrm{F}_4$ [4], Martoňák et al. compared the performance of Monte Carlo (MC) SA and path-integral Monte Carlo (PIMC) QA in simulating the ground state of the two-dimensional random Ising model. They found that QA outperformed SA in that case too [3]. Two years later, they found similar results when testing SA and QA on the Travelling Salesman Problem (TSP) [5].

The TSP is a famous CO problem. Given $N$ cities separated by distances $d_{ij}$, the goal is to find the shortest tour that visits each city exactly once and returns to the starting point. Instances of the TSP can be found in a range of areas, including supply chain optimisation, network routing, chip design, delivery planning and DNA sequencing. In this work, we restrict ourselves to the symmetric TSP, where we assert that the distance between two cities is the same in each direction, i.e. $d_{ij} = d_{ji}$ for all cities $i$ and $j$. The TSP is an NP-hard problem, meaning a solution can be verified in polynomial time, but finding the optimal solution likely scales exponentially with the size of the problem [1]. For a TSP with $N$ cities, there are $(N-1)!/2$ possible tours, making exhaustive search intractable for large $N$.

Whilst *ad-hoc* algorithms specifically tailored to the TSP are the most widely adopted, SA, due to its simplicity and flexibility, has been a consistently popular option for the TSP [6]. In this work, we follow in the footsteps of Martoňák et al., mapping the TSP to a two-dimensional Ising spin system for our implementation of Monte Carlo SA, and applying a Trotter decomposition for our implementation of PIMC QA. QA's superiority over SA for a small instance of the TSP is demonstrated. We go one step further and investigate how the performance of the two algorithms depends on their parameters, identifying ranges for each parameter that consistently and efficiently yield the most accurate results. Finally, we discuss the implications of our results to the field and suggest directions for future work in this area.

## II. TRAVELLING SALESMAN PROBLEM

Formally, for a TSP of $N$ cities, a valid tour can be represented by an $N \times N$ matrix $U$ of bits (1s and 0s), where

$$U_{ij} = U_{ji} = \begin{cases} 1 & \text{if } i \text{ and } j \text{ connected} \\ 0 & \text{otherwise.} \end{cases} \tag{1}$$

Since we are considering only the symmetric TSP, every valid tour has the same length as its reverse. As we will find out, it is convenient to use the above symmetric representation for undirected tours, i.e. $U = U^t$.

The total length of a tour $U$ is given by

$$L(U) = H_{\mathrm{pot}}(U) = \frac{1}{2}\sum_{i,j} d_{ij}U_{ij}, \tag{2}$$

where $d_{ij}$ is the distance between cities $i$ and $j$ as above. In the context of SA and QA, $H_{\mathrm{pot}}$ is the classical potential we seek to minimise.

[1] Until it is proven that $P \neq NP$, it is still possible that polynomial-time algorithms for NP-hard problems exist.

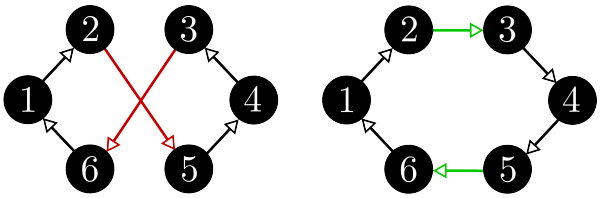


$$U = \begin{pmatrix} 0 & 1 & 0 & 0 & 0 & 1 \\ 1 & 0 & 0 & 0 & 1 & 0 \\ 0 & 0 & 0 & 1 & 0 & 1 \\ 0 & 0 & 1 & 0 & 1 & 0 \\ 0 & 1 & 0 & 1 & 0 & 0 \\ 1 & 0 & 1 & 0 & 0 & 0 \end{pmatrix} \qquad U' = \begin{pmatrix} 0 & 1 & 0 & 0 & 0 & 1 \\ 1 & 0 & 1 & 0 & 0 & 0 \\ 0 & 1 & 0 & 1 & 0 & 0 \\ 0 & 0 & 1 & 0 & 1 & 0 \\ 0 & 0 & 0 & 1 & 0 & 1 \\ 1 & 0 & 0 & 0 & 1 & 0 \end{pmatrix}$$

**FIG. 1:** Left: A six-city tour (`125436`) represented by symmetric matrix $U$. Right: The new tour (`123456`) obtained when a two-opt move on cities 2 and 3 is made, represented by symmetric matrix $U'$. Connections broken and created by the move are highlighted in red and green. Note that the move reverses the direction of the `345` sub-tour, but no bits (indicated by the red dashed circles) need to be flipped in our symmetric representation.

Both SA and QA rely on fluctuations to search the solution space and minimise length. To simulate such fluctuations, a *move* from the current configuration to a slightly different one is made. 2-opt, first proposed by Croes in 1958, is a simple local search algorithm often applied to the TSP [7]. For our fluctuations, we borrow the move from 2-opt. We break two existing connections $\{(i \to j), (k \to l)\}$ and form two new connections $\{(i \to k), (j \to l)\}$, to make a move to a new tour. Fig. 1 illustrates a 2-opt move on a simple six-city tour. We can see that making a 2-opt move in the symmetric tour representation is convenient as no bit-flips are necessary to account for the reversal of sub-tours. In the example move, the sub tour `543` is changed to `345` in the new tour, but the bits $U_{54}, U_{43}, U_{34}$ and $U_{45}$ (indicated by the red dashed circles) are unchanged.

## III. SIMULATED ANNEALING

In SA, thermal fluctuations are employed to stochastically sample the solution space $\{U\}$ according to an acceptance factor $P(\Delta H, T)$ that selects more harshly at lower temperatures. A popular choice of acceptance factor is the Metropolis criterion,

$$P(\Delta H, T) = \max\left[\exp\left(\frac{\Delta H}{T}\right), 1\right]. \tag{3}$$

Here, $\Delta H = (H_{\text{pot}}(U) - H_{\text{pot}}(U'))$ where the fluctuation is attempting to make a move from state $U$ to $U'$ and $T$ is the fictitious temperature gradually decreased from initial temperature $T_0$ to 0. The rate at which $T$ is decreased is the annealing schedule. Investigating different annealing schedules is a project in itself; in this work, we use a linear annealing schedule. At all values of $T$, the Metropolis criterion accepts any move that lowers the potential (i.e. $\Delta H > 0$). Moves that raise the potential are less likely to be accepted as $T$ is reduced [8]. As annealing progresses and $T$ is decreased, the system goes from sampling the full solution space with large thermal fluctuations to concentrating on sampling a smaller solution set in lower energy regions. As the annealing comes to an end, $T$ is low and the system is unable to overcome any potential barriers, instead tending towards its local minimum. In general, the final state is not the true ground state of $H_{\text{pot}}$, but, as we will see, it can come very close.

To implement SA, the standard Metropolis algorithm is employed. Initially, a random tour $U$ is generated and the system temperature is set to some $T_0$. Now, the annealing process begins: for $\tau$ Monte Carlo steps, a 2-opt move is applied to each of the $N$ cities, creating a new tour $U'$. The energy difference $\Delta H$ is then used to calculate the acceptance factor $P(\Delta H)$ (Eq. 3). A pseudo-random number $x$ between 0 and 1 is generated. If $P(\Delta H)$ is greater than $x$, then the current state $U$ is set to the new tour $U'$. If $P(\Delta H)$ is less than $x$, then the current state $U$ is kept the same. After each MC step, $T$ is updated according to the annealing schedule and the process is repeated. After $\tau$ MC steps, SA is complete and the final state $U$ is our best solution.

## IV. QUANTUM ANNEALING

Since we are making analogies to statistical physics, it makes sense to talk about the system in terms of spins. To a tour represented by symmetric matrix $U$, we associate a spin configuration

$$S^z_{ij} = S^z_{ji} = 2U_{ij} - 1 = \begin{cases} +1 & \text{if } i \text{ and } j \text{ connected} \\ -1 & \text{otherwise.} \end{cases} \tag{4}$$

In terms of spins, the classical potential in Eq. 2 becomes

$$H_{\text{pot}}(S) = \frac{1}{4}\sum_{i,j} d_{ij}\left(S^z_{ij} - 1\right). \tag{5}$$

We have mapped the TSP to an Ising-like system.

To induce the quantum fluctuations required for QA, we must introduce a kinetic energy term $H_{\text{kin}}$. As the TSP has no natural $H_{\text{kin}}$, we are left to devise one ourselves. Following the work of Martoňák et al., we again employ the 2-opt move. The 2-opt move $\{(i \to j), (k \to l)\} \to \{(i \to k), (j \to l)\}$ can be represented by spin operators,

$$S^+_{i,k} S^+_{j,l} S^-_{i,j} S^-_{k,l}, \tag{6}$$

where $S^{\pm}_{i,k}$ flips an Ising spin variable at $(i, j)$ and $(j, i)$.

We can now construct the quantum Hamiltonian for the TSP,

$$H_{\text{TSP}} = H_{\text{pot}}(U) + H_{\text{kin}}, \tag{7}$$

where we use the 2-opt spin operator representation to construct

$$H_{\text{kin}} = -\frac{1}{8}\Gamma(\tau)\sum_{(i,j)}\sum_{(k,l)} S^+_{i,k} S^+_{j,l} S^-_{i,j} S^-_{k,l}. \tag{8}$$

Here, $\Gamma(\tau)$ is a fictitious transverse magnetic field orthogonal to the Ising axis. A large initial $\Gamma_0$ is generally chosen so the kinetic energy term dominates at the start, providing the quantum fluctuations necessary to fully explore the solution space. As the annealing progresses, $\Gamma$ is carefully reduced, decreasing the contribution of the kinetic energy and enabling the quantum fluctuations to explore local solutions with lower potential. At all times, the Hilbert space

in which the tour matrices live is constrained, ensuring they always represent a valid tour.

While great strides have been made in building real-world quantum annealers over the last few decades, they are yet to reach the mainstream, so simulating QA on a classical computer remains desirable [9]. One approach is to evolve the system via numerical integration of the time-dependent Schrödinger equation, but this is extremely computationally intensive due to the size of the Hilbert space. Instead, we turn to the process of path-integral Monte Carlo (PIMC).

## V. PATH-INTEGRAL MONTE CARLO

To simulate QA with PIMC, we must first apply a Trotter discretisation to the path integral. For the $H_{\text{kin}}$ in Eq. 8, this is very difficult and would yield an 8-operator kinetic energy term. To preserve the simplicity of PIMC, we substitute our kinetic energy term with that of the standard transverse-field Ising model [10],

$$\tilde{H}_{\text{TSP}} = H_{\text{pot}}(S) - \Gamma(\tau) \sum_{(i,j)} S^{+}_{(i,j)}. \tag{9}$$

This Hamiltonian is trivially Trotter discretised. Strictly, the fluctuations due to this simplified kinetic energy term do not produce valid tours. However, by restricting ourselves to exclusively 2-opt moves, we ensure the constraints on the Hilbert space are always applied. Applying the Trotter breakup formula to the partition function of this transverse-field quantum Ising system, we find it is equivalent to the partition function of a classical Ising system with an extra dimension, referred to as the Trotter dimension. We can, therefore, map our quantum Ising system to a classical one with Hamiltonian given by

$$H^{P}_{TSP} = \sum_{k=1}^{P} \left( H_{\text{pot}} + J^{\perp} \sum_{(i,j)} S^{+,k}_{(i,j)} S^{+,k+1}_{(i,j)} \right), \tag{10}$$

where

$$J^{\perp} = -\frac{PT}{2} \ln \left( \tanh \frac{\Gamma}{PT} \right), \tag{11}$$

$T$ is the ambient temperature of our original quantum system and $PT$ is the temperature of our new classical system (Trotter temperature). A full derivation can be found in Ref. [3]. $P$ itself is called the Trotter number; as illustrated in Fig. 2, we can think of the new classical systems as $P$ slices of $N \times N$ spins arranged in parallel along the Trotter dimension, forming a 3-dimensional lattice. $J^{\perp}$ can be seen as an Ising-like coupling between equivalent spins in neighbouring Trotter slices [11]. If the intention was to simulate the exact quantum statistics of a system, we would have to work in the limit $P \to \infty$. Since, however, we are only interested in finding a state close to the classical ground state, we can work with finite $P$.

This mapping of a two-dimensional quantum system to a three-dimensional classical system allows us to simulate QA with a very similar standard Metropolis algorithm to that described in Section III with some small changes. Initially, when $\Gamma(\tau)$ is large, $J^{\perp}$ is very small and the interaction between Trotter slices is negligible. The 3-dimensional system resembles a set of $P$ isolated 2-dimensional systems. It is therefore appropriate to initialise the system as $P$ copies of a random tour. Again, the annealing process takes place over $\tau$ MC steps, for all of which $T$ is held constant. At each MC step, a 2-opt move is applied to each of the $N$ cities in each of the $P$ Trotter slices. Again, the acceptance factor in Eq. 3 is calculated using the Hamiltonian in Eq. 10 this time. After each MC step, $\Gamma$ is updated according to the annealing schedule. After $\tau$ MC steps, PIMC QA is complete and the Trotter slice with the lowest classical energy (Eq. 2) is taken as the best solution.

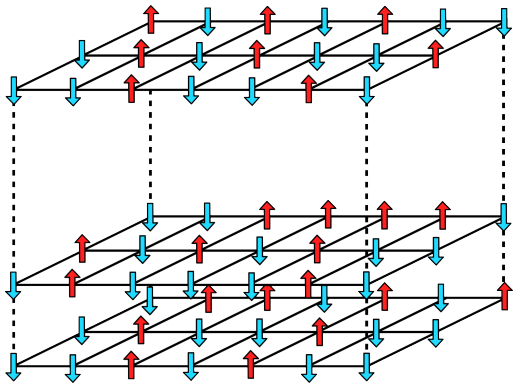

**FIG. 2:** An example of a 3-dimensional classical Ising system with Trotter slices stacked along the vertical Trotter axis. Three slices are indicated, but there are $P$ in total. The spins in neighbouring slices interact according to $J^{\perp}$. Note that each Trotter slice will have $N \times N$ spins arranged in a square lattice in our representation of the TSP.

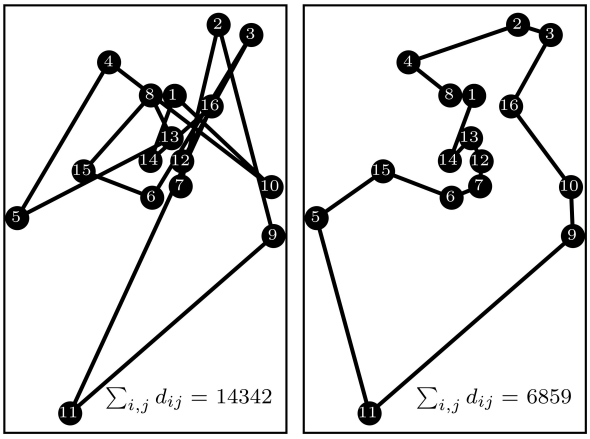


**FIG. 3:** Visualisation of the $N = 16$ instance `ulysses16` of `TSPLIB95`. Left: A random (and far from optimal) tour. Right: The optimal tour. The total length of each tour is indicated. Cities 11 and 13 have been slightly adjusted for clarity.

At each MC step in PIMC, $N \times P$ 2-opt moves are made. PIMC is, therefore, a factor of $P$ slower and requires a factor of $P$ more memory than SA. For a fair comparison of the algorithms, we introduce a quantity "total CPU time". For SA, this is just $\tau$. For PIMC, we account for the extra factor of $P$ and consider the product $\tau \times P$.

## VI. NUMERICAL IMPLEMENTATION

Both SA and QA were implemented in Python; their code has been made available in Ref. [12]. To compare the performance of SA and QA for the TSP, a small $N = 16$ city

instance of TSPLIB95, ulysses16, was selected [13]. ulysses16 is visualised in Fig. 3. On the left is a random, sub-optimal tour and on the right is the optimal tour with the problem's ideal length indicated. ulysses16 was chosen as it is both small enough that each algorithm could be run multiple times in the time available and large enough that the size of the solution space makes finding an accurate result a relatively difficult task.

Due to the probabilistic nature of Monte Carlo simulations, the solutions obtained by SA and QA vary when run multiple times. To capture the general performance of the algorithm, each simulation was repeated 20 times and the mean tour length $\bar{L}$ was calculated. A good algorithm must yield reliably accurate results; to quantify their uncertainty, the standard error was also calculated, see Appendix A.

The choice of parameters for SA and QA is an important and non-trivial task in its own right. In general, each instance of the TSP has a unique set of parameters that yield the best results. Initially, we identified, via trial and error, $\tau = 100$, $P = 10$, $\Gamma_0 = 300$ and $PT = 50$ to be values that yield good results efficiently. To determine their optimal values for solving ulysses16, trials were run varying one quantity at a time. We expect the performance of each algorithm to show a strong dependence on the choice of parameters. The choice of $\Gamma_0$ is expected to be more arbitrary as long as it is sufficiently greater than the $d_{ij}$. For both SA and QA, a linear annealing schedule was used.

## VII. RESULTS AND DISCUSSION

We quantify the success of the SA and QA by the mean excess lengths between the length of the obtained tours and the optimal tour,

$$\bar{\epsilon}_{\text{exc}} = \frac{\bar{L} - L_{\text{opt}}}{L_{\text{opt}}}, \tag{12}$$

where $\bar{L}$ is as defined above and $L_{\text{opt}}$ is the total length of the optimal tour. To investigate the dependence of SA and QA on parameter choice, $\bar{\epsilon}_{\text{exc}}$ was plotted against each parameter individually. For a quantitative comparison of SA and QA, the dependence of $\bar{\epsilon}_{\text{exc}}$ as a function of $\tau$ was studied.

### A. Dependence of SA and QA on parameter choice

As described in Section III, $T$ governs the extent to which SA samples the full solution space. Therefore, we expect SA run from a low initial temperature $T_0$ to get stuck in local minima. In contrast, for high values of $T_0$, we expect SA to continue to sample the whole solution space for the whole annealing process, meaning it never converges on the shortest paths. In Fig. 4, $\bar{\epsilon}_{\text{exc}}$ was plotted (black, filled circles) for values of $T_0$ ranging from 1 to 400. As expected, SA performed less well at low and high values of $T_0$. SA performed best when $T_0$ was around 50.

We saw in Section V that, in QA, the strength of the coupling $J^{\perp}$ between spins in neighbouring Trotter slices is determined, for a given $\Gamma$, by the Trotter temperature $PT$. By definition, the Trotter number $P$ itself governs the number of slices in the Trotter axis. Therefore, it makes sense to

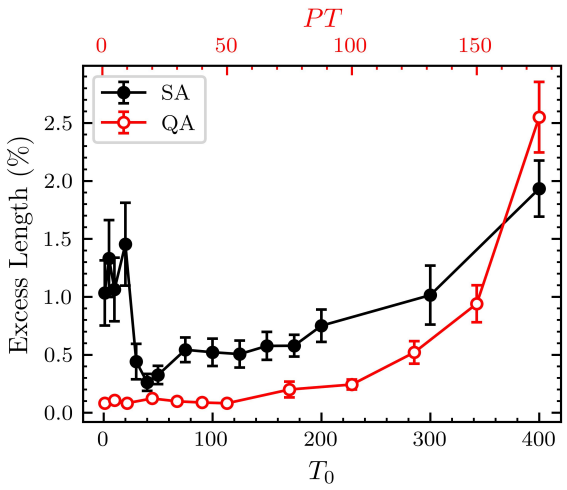


**FIG. 4:** Excess length as a percentage of the optimal length after simulated annealing (SA) from initial temperatures $T_0$ and quantum annealing (QA) at $PT$, averaged over 20 runs, for the $N = 16$ instance ulysses16 of TSPLIB95. In each case, the total number of Monte Carlo steps $\tau$ was 100 and QA was carried out with a $\Gamma_0$ of 300 and a $P$ of 10.

investigate the dependence of $\bar{\epsilon}_{\text{exc}}$ on both $PT$ and $P$ independently. In Fig. 4, $\bar{\epsilon}_{\text{exc}}$ was plotted (red, open circles) for values of $PT$ ranging from 1 to 175. In the range studied, $\bar{\epsilon}_{\text{exc}}$ more or less increased with $PT$. At high $PT$, $H_{\text{pot}}$ is negligible compared to $J^{\perp}$ throughout the annealing. Instead of converging on the minimum of the potential, the system minimises the interactions between adjacent Trotter slices and ends up with $P$ copies of the same tour, yielding a large, uncertain $\bar{\epsilon}_{\text{exc}}$. For all values below 100, the system converged on the optimal tour. This is surprising and doesn't match the results found in the literature, where QA fails to converge for low values of $PT$ [3]. In the limit $PT \to 0$, $J^{\perp} \sim 0$ and the process is essentially SA with an extra factor of $P$ moves every MC step. We will see that QA outperforms SA at equivalent CPU time if the total $\tau$ is greater than 500. Accounting for the extra factor of $P$ here, at low $PT$ our QA is essentially SA with a total CPU time of 1000, so we would expect to see an increase in $\bar{\epsilon}_{\text{exc}}$. We suspect that studying this further with larger instances of the TSP, where the superiority of QA is more apparent, would yield the expected results.

In Fig. 5, $\bar{\epsilon}_{\text{exc}}$ was plotted for values of $P$ between 1 and 30. $\bar{\epsilon}_{\text{exc}}$ for each $P$ was under $0.2\%$, decreasing as $P$ increased up to 20 and staying roughly the same for 20 and 30. The uncertainty followed a similar trend, decreasing as $P$ increased up to 20 and increasing slightly between 20 and 30. These results matched the theory: at low $P$, QA approaches SA. For larger problems than ulysses16, we expect to notice a decrease in $\bar{\epsilon}_{\text{exc}}$ as $P$ increases beyond 20.

In Fig. 6, $\bar{\epsilon}_{\text{exc}}$ was plotted for initial transverse field strength $\Gamma_0$ ranging from 1 to 500. As predicted in Section VI, increasing $\Gamma_0$ beyond a certain value had little effect on the performance of QA. For values over 300, the algorithm performed accurately and with little uncertainty. At low values of $\Gamma_0$, the quantum fluctuations are too small to explore the full solution space, leading to high excess lengths with significant uncertainty.

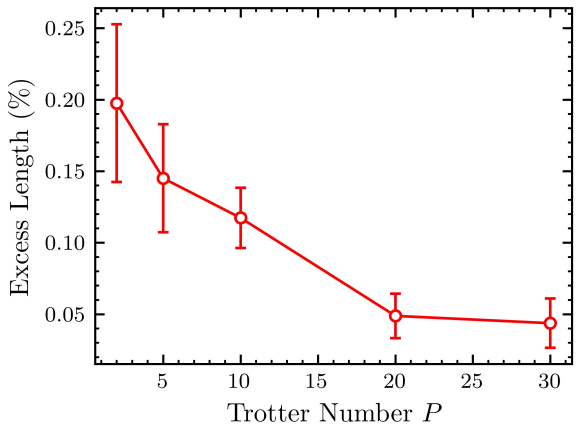


**FIG. 5:** Excess length as a percentage of the optimal length after quantum annealing (QA) with Trotter number $P$, averaged over 20 runs, for the $N = 16$ instance `ulysses16` of `TSPLIB95`. In each case, $\Gamma_0$ was 300, $PT$ was 50 and $\tau$ was 100.

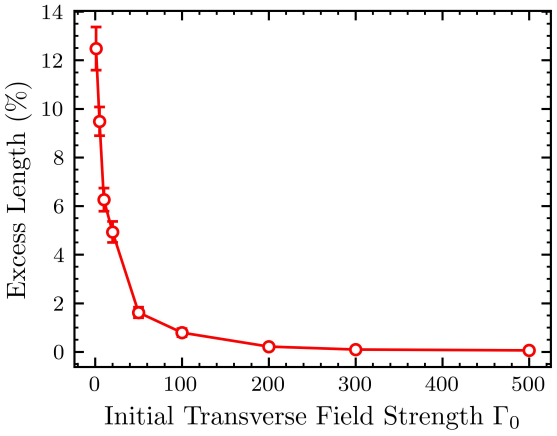


**FIG. 6:** Excess length as a percentage of the optimal length after quantum annealing (QA) with initial transverse field strength $\Gamma_0$, averaged over 20 runs, for the $N = 16$ instance `ulysses16` of `TSPLIB95`. In each case, $P$ was 10, $PT$ was 50 and $\tau$ was 100.

### B. Comparison between SA and QA

To compare SA and QA, we studied their performance for $\tau$ ranging from 25 to 1000. Fig. 7 shows the $\bar{\epsilon}_{\text{exc}}$ obtained in each case. Also indicated (blue, open circles) is the excess length after QA for $\tau$ MC steps plotted against $\tau \times P$, enabling a direct comparison between SA and QA for equivalent total CPU time. For all $\tau$ investigated and both algorithms, results obtained were within $1.2\%$ of the optimal length. For SA and QA, the uncertainty decreased, in general, as $\tau$ increased. If $\bar{\epsilon}_{\text{exc}}$ less than $0.2\%$ is desired, or CPU time is greater than 500, QA is superior to SA.

These results closely resemble those of Martoňák et al. for a larger $N = 1002$ TSP instance, `pr1002`, and for the two-dimensional random Ising model [3, 5]. They support the theory that the ability of quantum systems to tunnel out of local minima enables QA to converge to an approximate ground state more quickly than SA.

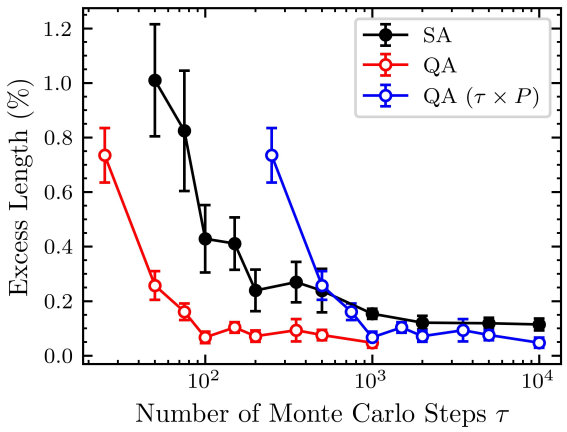


**FIG. 7:** Excess length as a percentage of the optimal length after simulated annealing (SA) and quantum annealing (QA) for total Monte Carlo steps $\tau$, averaged over **3** runs, for the $N = 16$ instance `ulysses16` of `TSPLIB95`. In each case, SA was carried out with $T_0 = 100$ and QA was carried out with $\Gamma_0 = 300$, $PT = 100$ and $P = 10$.

## VIII. CONCLUSION AND OUTLOOK

In this report, we have investigated the applicability of quantum annealing simulated with the path-integral Monte Carlo technique as a combinatorial optimisation algorithm, with the Travelling Salesman Problem as an example test. We compared it to simulated annealing, an established algorithm for combinatorial optimisation, demonstrating its superiority in producing accurate results efficiently. Whilst SA has never been the most popular TSP algorithm, being beaten consistently by others specifically tailored to the problem, the success of QA in these tests encourages future research into its application as another general-purpose CO algorithm. Moreover, it would be interesting to see how QA performs on other, real-world CO problems, such as those in computational biology described by Greenberg et al. [14].

Since Martoňák et al. published their work on quantum annealing the TSP in 2002, there have been many developments in the field. Researchers have found success in combining QA with a range of classical heuristics, and other hybrid quantum-classical algorithms such as the quantum approximate optimisation algorithm (QAOA), introduced by Farhi et al. in 2014, where the problem is encoded into a quantum circuit, on which classical optimisation algorithms are applied iteratively until the system converges to a near-optimal solution [15, 16]. It would be interesting to implement some of these algorithms and compare their performance to QA for the TSP.

As mentioned before, some success has been found in building real-world quantum annealers. Whilst they are still some way away from beating classical computers as the hardware of choice for CO and struggle to solve even simple instances of the TSP [17], they remain an active and interesting area of research.

This work was somewhat limited by available time and computing power. Given more of each, it would be interesting to study the performance of QA as a function of its parameters for a large set of TSPs of various sizes. Such a study could enable the writing of a guide for QA parameter selection, allowing QA to be applied to a broader range of problems.

Numerically, our implementation of PIMC was relatively basic. There is clear scope for efficiency improvements: running each Trotter slice in parallel would yield a significantly faster algorithm, as would simplifying the energy difference calculation to only consider change due to the four spins flipped in each move.

## REFERENCES


[1] Fernando Peres and Mauro Castelli. Combinatorial optimization problems and metaheuristics: Review, challenges, design, and development. 11(14):6449. ISSN 2076-3417. doi: 10.3390/app11146449. URL https://www.mdpi.com/2076-3417/11/14/6449. Number: 14 Publisher: Multidisciplinary Digital Publishing Institute.

[2] S. Kirkpatrick, C. D. Gelatt, and M. P. Vecchi. Optimization by simulated annealing. 220(4598):671–680. doi: 10.1126/science.220.4598.671. URL https://www.science.org/doi/10.1126/science.220.4598.671. Publisher: American Association for the Advancement of Science.

[3] Roman Martoňák, Giuseppe E. Santoro, and Erio Tosatti. Quantum annealing by the path-integral monte carlo method: The two-dimensional random ising model. 66(9):094203. doi:10.1103/PhysRevB.66.094203. URL https://link.aps.org/doi/10.1103/PhysRevB.66.094203. Publisher: American Physical Society.

[4] J. Brooke, D. Bitko, T. F. Rosenbaum, and G. Aeppli. Quantum annealing of a disordered magnet. URL http://arxiv.org/abs/cond-mat/0105238.

[5] Roman Martonak, Giuseppe E. Santoro, and Erio Tosatti. Quantum annealing of the traveling salesman problem. 70(5):057701. ISSN 1539-3755, 1550-2376. doi: 10.1103/PhysRevE.70.057701. URL http://arxiv.org/abs/cond-mat/0402330.

[6] Y. Crama, A. W. J. Kolen, and E. J. Pesch. Local search in combinatorial optimization. In P. J. Braspenning, F. Thuijsman, and A. J. M. M. Weijters, editors, Artificial Neural Networks: An Introduction to ANN Theory and Practice, Lecture Notes in Computer Science, pages 157–174. Springer. ISBN 978-3-540-49283-2. doi: 10.1007/BFb0027029. URL https://doi.org/10.1007/BFb0027029.

[7] G. A. Croes. A method for solving traveling-salesman problems. 6(6):791–812. ISSN 0030-364X. URL https://www.jstor.org/stable/167074. Publisher: INFORMS.

[8] Tadashi Kadowaki. Study of optimization problems by quantum annealing. URL http://arxiv.org/abs/quant-ph/0205020.

[9] What is quantum annealing? — d-wave system documentation documentation. URL https://docs.dwavesys.com/docs/latest/c_gs_2.html#getting-started-qa.

[10] Lorenzo Stella. Studies of classical and quantum annealing. URL https://iris.sissa.it/handle/20.500.11767/4079.

[11] Masuo Suzuki. Relationship between d-dimensional quantal spin systems and (d+1)-dimensional ising systems: Equivalence, critical exponents and systematic approximants of the partition function and spin correlations. 56(5):1454–1469. ISSN 0033-068X. doi:10.1143/PTP.56.1454. URL https://doi.org/10.1143/PTP.56.1454.

[12] Frederick Bullard. pimc. URL https://github.com/fs-bullard/pimc. original-date: 2024-01-19T10:39:14Z.

[13] Gerhard Reinelt. TSPLIB. URL http://comopt.ifi.uni-heidelberg.de/software/TSPLIB95/.

[14] H.J. Greenberg, W.E. Hart, and G. Lancia. Opportunities for combinatorial optimization in computational biology. 16(3):211–231. ISSN 1091-9856. doi:10.1287/ijoc.1040.0073.

[15] Nicholas Chancellor. Modernizing quantum annealing using local searches. 19(2):023024. ISSN 1367-2630. doi: 10.1088/1367-2630/aa59c4. URL http://arxiv.org/abs/1606.06833.

[16] Edward Farhi, Jeffrey Goldstone, and Sam Gutmann. A quantum approximate optimization algorithm. URL http://arxiv.org/abs/1411.4028.

[17] Siddharth Jain. Solving the traveling salesman problem on the d-wave quantum computer. 9. ISSN 2296-424X. doi: 10.3389/fphy.2021.760783. URL https://www.frontiersin.org/articles/10.3389/fphy.2021.760783. Publisher: Frontiers.

### Appendix A: Errors

The error in excess length $\alpha_\epsilon$ indicated in Figs. 4 to 7, is the standard error over the population of 20 runs for each mean, given by

$$\alpha_\epsilon = \frac{\sigma_\epsilon}{\sqrt{20}}, \tag{A1}$$

where

$$\sigma_\epsilon = \sqrt{\frac{1}{20}\sum_{i=1}^{20}(\epsilon_i - \bar{\epsilon})^2}. \tag{A2}$$

**SCIENTIFIC SUMMARY FOR A GENERAL AUDIENCE**

A salesman planning a route visiting several cities and a computer chip designer arranging components on a chip face a common challenge: finding a route between points that minimises cost. This puzzle is found in various fields, from logistics to tourism, and is known as the Travelling Salesman Problem (TSP).

One way to solve the TSP is to list every possible route and choose the shortest one. Unfortunately, for complex problems with many points, the number of possible routes is extremely large, making this approach impractical. Instead, we turn to more sophisticated methods such as simulated annealing (SA) and quantum annealing (QA).

Picture, as below, the TSP as a landscape with hills and valleys, where hills represent longer routes and valleys represent shorter ones. With SA, we attempt to find the lowest valley by jumping randomly from spot to spot, comparing one spot with the next. QA, however, employs a quantum phenomenon called tunnelling, allowing us to '*teleport*' through hills to reach the bottom faster.

In this report, we demonstrate that QA solves the TSP more efficiently than SA, suggesting that QA holds potential for cost-reduction in real-world instances of the Travelling Salesman Problem.